Colloid Polym Sci (2004) 282: 844–853
DOI 10.1007/s00396-004-1130-3

ORIGINAL CONTRIBUTION

Lidia Okrasa
Tadeusz Pakula
Yoshihisa Inoue
Krzysztof Matyjaszewski

Morphology and thermomechanical properties of well-defined polyethylene-*graft*-poly(*n*-butyl acrylate) prepared by atom transfer radical polymerization

Received: 29 March 2004
Accepted: 5 April 2004
Published online: 5 May 2004

Dedicated to Prof. E. W. Fischer on the occasion of his 75th birthday

L. Okrasa · T. Pakula (✉)
Max-Planck-Institute for Polymer Research,
Postfach 3148, 55021 Mainz,
Germany
E-mail: tadeusz.pakula@mpip-mainz.mpg.de

Y. Inoue · K. Matyjaszewski
Center for Macromolecular Engineering,
Department of Chemistry,
Carnegie Mellon University,
4400 Fifth Avenue,
Pittsburgh, Pennsylvania
15213, USA

Present address: L. Okrasa
Department of Molecular Physics,
Technical University of Lodz,
Lodz, Poland

Abstract The morphology and thermomechanical properties of well-defined polyethylene-*graft*-poly(*n*-butyl acrylate) (PE-*g*-PBA) copolymers prepared via atom transfer radical polymerization were investigated. Differential scanning calorimetry (DSC), small angle X-ray scattering (SAXS), wide angle X-ray scattering (WAXS), dynamic mechanical measurement and large deformation tensile tests were performed on the graft copolymers and the results were compared with the behavior of the polyethylene macroinitiator. The existence of both crystalline polyethylene segments and amorphous poly(*n*-butyl acrylate) segments in the copolymers leads to microphase separation and unique thermomechanical behavior. Strong microphase separation was observed by DSC and X-ray diffraction studies. Correlation of morphology and thermomechanical properties was also studied using dynamic mechanical measurement and large deformation tensile tests.

Keywords Grafted copolymers · ATRP · Morphology · X-ray scattering · Mechanical properties

Introduction

The preparation of block and graft copolymers has been extensively studied in polymer science because of the range of properties attainable in such materials and the variety of applications whose requirements can be met by selecting the composition of the copolymer segments. One advantage of such segmented copolymers is that it is possible to incorporate two or more polymer segments each having totally different chemical or physical properties into one polymer chain. A broad range of polymer properties can be designed and tailored into the copolymers by changing monomers, chain length of each segment and topology. Among such copolymers, polyolefin segmented block and graft copolymers have been targeted [1, 2] because, although polyolefins are the largest volume of commercially produced thermoplastics, the incorporation of polar segments would further enhance their properties and dramatically extend their utility in a number of applications.

While several methods have been used to synthesize such segmented copolymers, controlled/''living'' radical

polymerization (CRP) [3, 4, 5, 6] is presently the most versatile technology that can be employed to synthesize well-defined block and graft copolymers. A wide spectrum of segmented copolymers has been synthesized via CRP. Among the several CRP techniques that have been developed, atom transfer radical polymerization (ATRP) [7, 8, 9, 10, 11, 12, 13, 14, 15, 16, 17, 18, 19] is the most promising method due to its availability, versatility and low catalyst cost. So far, a range of polyolefin segmented copolymers have been successfully synthesized via ATRP. The copolymers include blocks copolymers [20, 21, 22, 23, 24, 25], graft copolymers having polyolefin main chain [26, 27, 28, 29, 30] and graft copolymers with polyolefin side chains [31]. A graft copolymer with polyolefin side chain was also synthesized via nitroxide-mediated polymerization [32].

As noted above, the synthesis of several examples of block and graft copolymers have been reported; however the majority of the materials have amorphous polyolefin segments, e.g., branched polyethylene, ethylene/α-olefin copolymer, atactic polypropylene or polyisobutene. There are few examples of block and graft copolymers with crystalline polyolefin segments, such as linear polyethylene or isotactic polypropylene [22, 23, 29]. This is probably due to the difficulties associated with the synthesis of functional polyolefins and the low solubility of polyolefin macroinitiators, or macromonomers, under conditions suitable for CRP. Therefore, the synthesis of block [23] and graft [33] copolymers having both linear polyethylene segments and polar polymer segments, e.g., poly(meth)acrylate segments was targeted. Previously, we reported the synthesis of polyethylene-*graft*-poly(*n*-butyl acrylate), (PE-*g*-PBA), from a multifunctional polyethylene macroinitiator via ATRP of *n*-butyl acrylate [33]. This graft copolymer possessed a linear PE main chain and PBA side chains, i.e., crystalline nonpolar segments and amorphous polar segments. The PBA side chains were grown from the macroinitiator under well controlled ATRP conditions, and the chain length can be easily changed by changing polymerization time. We further decided to investigate the morphology and thermomechanical properties of these PE-*g*-PBA copolymers to develop an understanding of the correlation between microstructure and physical properties in graft copolymers having such totally different segments.

In this paper, the morphology and thermomechanical properties of PE-*g*-PBA copolymers were investigated using differential scanning calorimetry (DSC), small angle X-ray scattering (SAXS), wide angle X-ray scattering (WAXS), mechanical spectroscopy and large deformation tensile tests. The investigation suggested strong microphase separation in the graft copolymers. Unique thermomechanical properties were observed as a result of the microphase separation.

Experimental

Characterization ^{1}H NMR spectra of the polyethylene multifunctional macroinitiator (PE-macroinitiator) in *o*-dichlorobenezene-d_4 was recorded at 120 °C using a 400-MHz JEOL JNM GSX400. The molecular weight and molecular weight distribution of the PE-macroinitiator were determined by high temperature GPC using a Waters 150-C gel permeation chromatograph equipped with three TSKgel columns (two sets of TSKgelGMH_{HR}-H(S)HT and one TSKgelGMH_6-HTL) at 145 °C. GPC was performed using *o*-dichlorobenzene as eluent at the flow rate of 1 mL/min. Universal calibration technique was used to determine the molecular weight and molecular weight distribution of the PE-macroinitiator. Conversion of *n*-butyl acrylate monomer was determined by gas chromatography using a Shimadzu GC 14-A gas chromatograph equipped with a FID detector and J&W Scientific 30-m DB WAX Megabore column. The molecular weight and molecular weight distribution of the detached poly(*n*-butyl acrylate) side chains were determined by GPC using PSS column (styrogel 10^5, 10^3, 10^2 Å) with RI detectors. GPC was performed using THF as the eluent at the flow rate of 1 mL/min. Linear polystyrene standards were used for calibration of poly(*n*-butyl acrylate).

Materials Ethylene was purchased from Sumitomo Seika Co. Ltd. Methylaluminoxane (MAO) was purchased from Albemarle as a 20% toluene solution and the remaining trimethyl aluminum was removed under vacuum before use. Zirconium metallocene complex was prepared as reported previously [34]. Toluene was dried over Al_2O_3. Copper (I) chloride [35] and tris(2-(di(2-(*n*-butoxycarbonyl)ethyl)amino)ethyl)amine (BA_6TREN) [36] were purified and prepared as detailed in previous reports. *n*-Butyl acrylate (BA) was passed through a neutral alumina column to remove stabilizer, dried over calcium hydride and distilled under reduced pressure before use. All other reagents and solvents were used as received.

ATRP of n-butyl acrylate from a PE multifunctional macroinitiator A polyethylene multifunctional macroinitiator (PE-macroinitiator), $M_n = 36000$, $M_w/M_n = 3.04$ with 0.90 mol% of α-bromoisobutyrate functionality, was synthesized as reported previously [33]. ATRP was performed using standard Schlenk techniques. Solvents and monomers were degassed through bubbling with nitrogen for 30 min prior to use. A catalyst stock solution was prepared by dissolving CuCl (31.2 mg, 3.15×10^{-4} mol), $CuCl_2$ (2.1 mg, 1.56×10^{-5} mol), and BA_6TREN (301.8 mg,

3.30×10^{-4} mol) in chlorobenzene (5 mL). Separately, the PE-macroinitiator (119.1 mg, 3.49×10^{-5} mol-Br) was placed in a 25 ml Schlenk flask and then BA (0.5 mL, 3.49×10^{-3} mol), chlorobenzene (1.8 mL), anisole (0.1 mL), and catalyst stock solution, (0.59 ml, 3.51×10^{-5} mol-CuCl/BA_6TREN, 1.74×10^{-6} mol-$CuCl_2$/BA_6TREN) were successively added to the flask. The resulting mixture was warmed up to 100 °C to start the polymerization, the PE-macroinitiator dissolved in the solvent/monomer mixture within a few minutes. Polymerization was stopped after 0.5, 1.0, or 3.75 h, and the resulting graft copolymer was precipitated in excess methanol. The graft copolymers were filtrated, washed with methanol and dried under vacuum at 60 °C.

Side chain cleavage and analysis The graft copolymer (30 mg) was dissolved in chlorobenzene (1 mL) at 100 °C. *n*-Butanol (4 mL) and H_2SO_4 (three drops) were added to the solution and the resulting mixture was stirred at 100 °C for three days. After cooling, OH type anionic ion exchange resin was added to neutralize the acid catalyst, and then the solution was decanted from the ion-exchange resin. After evaporation of solvent, the remaining polymer was extracted with THF, and GPC of side chain PBA was taken using THF GPC.

Differential scanning calorimetry (DSC) DSC measurements were performed on a Mettler DSC 30 apparatus at a temperature variation rate of 10 °C/min for both heating and cooling runs. The reported transition temperatures and melting enthalpies were taken from the second heating run.

Small angle (SAXS) and wide angle (WAXS) X-ray scattering Small angle (SAXS) and the wide angle (WAXS) scattering techniques have been used to characterize the structure of bulk copolymers. WAXS measurements have been performed using a θ–θ diffractometer (Simens) as well as a 2D position sensitive detector with a pin-hole collimation of the incident beam. Cu Kα radiation ($\lambda = 0.154$ nm) was used. For the SAXS measurements a rotating anode X-ray source with a pin-hole beam collimation and a 2D position sensitive detector were used. Measurements have been performed at room temperature and at a temperature above the melting point of the PE phase (150 or 170 °C). The recorded scattered intensity distributions are presented as functions of the scattering vector ($s = 2\sin\theta/\lambda$, where 2θ is the scattering angle).

Dynamic mechanical measurements The mechanical characterization has been performed using the ARES mechanical spectrometer (Rheometric Scientific). Shear deformation has been applied under condition of controlled deformation amplitude, always remaining in the range of the linear viscoelastic response of studied samples. Geometry of parallel plates has been used with plate diameters of 6 mm. The gap between plates (sample thickness) was about 1 mm. Experiments have been performed under dry nitrogen atmosphere. Temperature dependencies of the real, G′, and imaginary, G″, parts of the complex shear modulus were determined at a constant deformation frequency of 10 rad/s under continuous cooling of samples with the rate of 2 °C/min. The dependencies are used to characterize the properties within the broad temperature range extending between −100 °C and 180 °C.

Large deformation tensile tests Measurements were performed using a mechanical testing machine Instron 6000. Samples having the thickness of about 0.2 mm have been drawn with the rate of 0.5/min at room temperature. Dependencies of stress vs draw ratio were recorded. Elastic modulus (E) and the coordinates of the yield point (λ_Y, σ_Y) as well as of the point of fracture (λ_B, σ_B) have been determined as averages of 3–5 independent drawing experiments performed at the same conditions. The meaning of the parameters determined is illustrated in Fig. 1. Only the room temperature behavior is reported.

Results and discussions

Synthesis of polyethylene-graft-poly(*n*-butyl acrylate)

The synthetic route to PE-*g*-PBA is illustrated in Scheme 1. As reported previously [33], ethylene and 10-undecen-1-ol were copolymerized in the presence of triethylaluminum catalyzed by zirconium metallocene

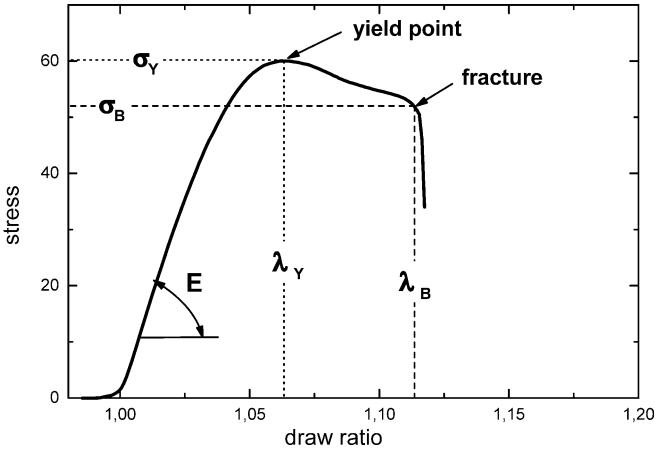

Fig. 1 Schematic stress-strain dependence with the parameters characterizing the elasticity at small deformation as well as the yield and the break points

Scheme 1 Synthetic route for PE-*g*-PBA

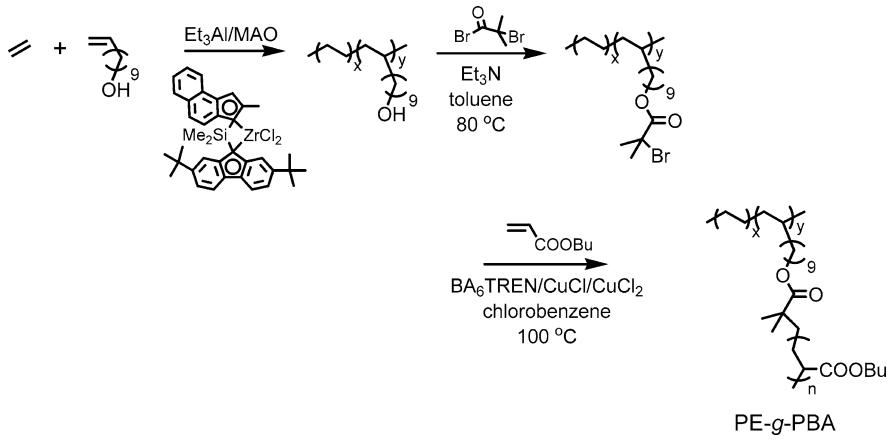

catalyst and methylaluminoxane (MAO). The hydroxy functionality in the resulting poly(ethylene-*co*-10-undecen-1-ol) was converted into α-bromoisobutyrate functionality through reaction with α-bromoisobutyryl bromide in the presence of triethylamine. The reaction proceeded quantitatively and the desired PE-macroinitiator was obtained ($M_n = 36{,}000$, $M_w/M_n = 3.04$, 0.90 mol% of ATRP functionality) [33].

PE-*g*-PBA copolymers were synthesized using this PE-macroinitiator under the same ATRP conditions reported earlier [33]. BA polymerization was conducted using $CuCl/CuCl_2/BA_6TREN$ as catalyst at 100 °C. The key to success for this "grafting from" polymerization was low monomer concentration, halogen exchange technique, addition of copper(II) and use of BA_6TREN as ATRP ligand. Under these conditions undesired radical coupling termination reactions were minimized and growth of the PBA side chains was well controlled, while polymerization rate was sufficiently fast. Graft copolymers with DP of the side chains = 13, 33, and 51 were obtained by simply changing polymerization time. Well-controlled polymerizations were confirmed through analysis of the PBA side chain by GPC after defacement from the PE main chain through a transesterification reaction using *n*-butanol catalyzed H_2SO_4, as reported before [33]. The results are summarized in Table 1.

Morphology and thermo-mechanical properties of PE-*g*-PBA.

A comprehensive analysis of morphology and thermo-mechanical properties of these well-defined graft copolymers was performed. The bulk polyethylene macroinitiator sample (PE-M) was used as a reference material and has been analyzed in the same way as the grafted copolymers. Both in the reference sample and in the grafted copolymers a semicrystalline character has been observed. The DSC thermograms revealed clear melting and crystallization peaks related to the PE fraction, as illustrated in Fig. 2 by means of the traces recorded under heating and cooling, respectively. The parameters of the transitions observed in these samples using the DSC method are listed in Table 2. The melting enthalpy and the melting temperature decrease considerably with the increase of the volume fraction of the PBA. The melting enthalpies allow an estimation of crystallinity degrees, Xc ($= \Delta H/\Delta H° \times 100$, where $\Delta H°$ represents the hypothetical enthalpy of the 100% crys-

Table 1 PE-macroinitiator and PE-*g*-PBA copolymers via ATRP[a]

Sample no.	Polymer	PBA side chain					
		DP[b]	M_n[c]	$M_{n,\ theo}$[c]	M_w[c]	M_w/M_n[c]	Weight fraction[d]
PE-M	PE-macroinitiator[e]	0					0
GR1	PE-*g*-PBA	12.6	1720	1840	2450	1.43	0.321
GR2	PE-*g*-PBA	33.4	3650	4500	4990	1.37	0.556
GR3	PE-*g*-PBA	51.1	6320	6770	8420	1.33	0.657

[a]Polymerization conditions: $[BA]_0/[PE\text{-}M]_0/[CuCl]_0/[CuCl_2]_0/[BA_6TREN]_0 = 100/1/1/0.05/1.05$; $[BA]_0 = 1.16$ mol/L; solvent = chlorobenzene; initiator = PE-multifunctional macroinitiator; T = 100 °C, t = 0.5 h (GR1), 1.0 h (GR2), and 3.75 h (GR3)
[b]Based on monomer conversion
[c]PBA side chain after detached from main chain
[d]Calculated based on monomer conversion
[e]$M_n = 36{,}000$, $M_w = 109{,}300$, $M_w/M_n = 3.09$, 0.90 mol% α,ω-unsaturated ester group was incorporated

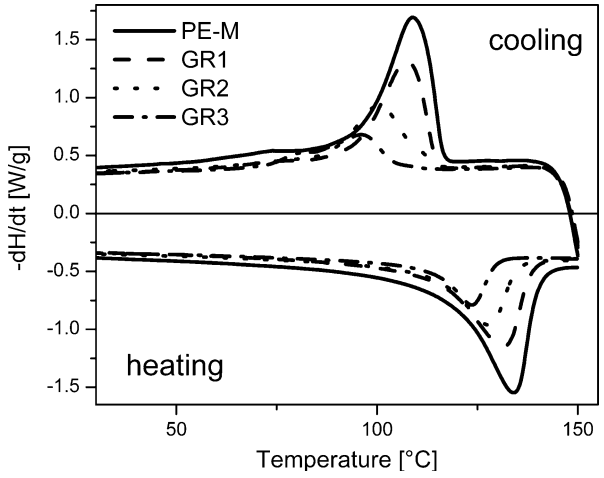

Fig. 2 DSC thermograms recorded during cooling and heating with the rate 10 °C/min for the PE macroinitiator and PE-*g*-PBA polymers

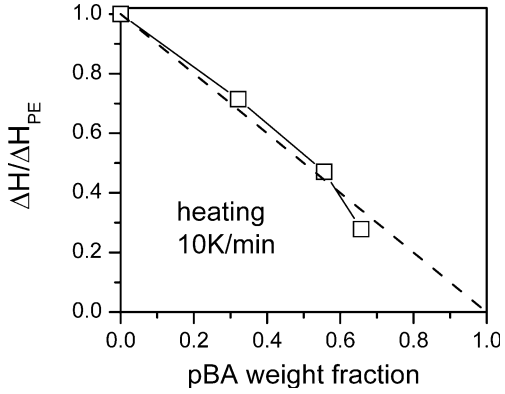

Fig. 3 Normalized melting enthalpy vs composition for the polymers with various lengths of grafted chains

talline sample). The values determined in this way (Table 2) show that even for the macroinitiator the crystallinity is rather low which should be attributed to a relatively frequent branching of the polyethylene backbone. Nevertheless, the crystallization ability of the PE seems to be only weakly influenced by the increasing lengths of the grafted non-crystallizable chains, illustrated by rather small shifts of the maxima in the cooling curves towards lower temperatures.

Indeed, the variation of the melting enthalpies with composition for the studied samples seems to be directly related to the volume fraction of the crystallizing component. This is illustrated in Fig. 3 where the melting enthalpy of the grafted polymers normalized by the value determined for the PE macroinitiator sample is plotted vs composition. At least up to the composition 0.5, the fraction of the crystalline phase is nearly proportional to the PE content in the material.

For the grafted polymers, glass transitions corresponding to the PBA phase were detected in the DSC thermograms (see Fig. 4). The T_g values determined are listed in Table 2. Independent of composition, the temperatures of the transition were not significantly different from values characteristic for bulk PBA material which suggests a strong microphase separation between PBA side chains and PE backbone. The glass transition corresponding to the PE phase was not detectable in the DSC traces recorded in the temperature range extending down to −150 °C.

The X-ray diffraction intensity distributions recorded for the studied samples using the θ–θ diffractometer are shown in Fig. 5. The results are obtained both at room temperature and at 170 °C, i.e., below and above the melting point of the polyethylene fraction, respectively. The presence of crystallinity is confirmed by the room temperature results, in which the three intensity peaks characteristic for the orthorhombic polyethylene unit cell are observed (corresponding to 110, 200, and 020 planes in the order of increasing s) with intensities decreasing with the increasing length of the PBA side chains. The variation of composition in the studied samples is also related to variation of intensity of a broad low angle halo which is not present in the polyethylene sample but appears with increasing intensity for samples with longer side chains. This halo is characteristic for the X-ray diffraction on bulk PBA and is attributed to the backbone-backbone correlation in this polymer. The presence of the halo in the grafted polymers indicates that the PE and PBA macromolecular fragments remain phase separated both in the amorphous regions of the semicrystalline copolymer state and in the melt at the temperature well above the melting point of the polyethylene (Fig. 5b).

The multiphase structure of the studied polymers is also detected by means of the small angle X-ray scattering. The results of the scattered intensity distributions recorded at temperatures below and above the melting

Table 2 Transition temperatures and melting enthalpies determined from the DSC thermograms

Sample	PBA wt. fract.	T_m [°C]	ΔH[J/g]	$\Delta H/\Delta H_{PE}$	Xc [%][a]	T_c [°C]	T_g[°C]
PE-M	0	132.4	108.9	1	37.5	108.9	-
GR1	0.321	130	77.8	0.71	26.8	107.2	−43.6
GR2	0.556	126.6	51.3	0.47	17.7	100.4	−45.3
GR3	0.657	122.8	30.3	0.28	10.5	95.4	−44.9

[a] $c = \Delta H/\Delta H° \times 100$, where $\Delta H° = 290.4$ J/g [37]

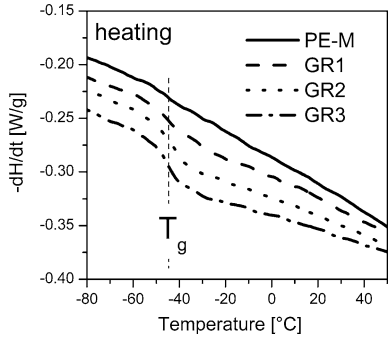

Fig. 4 Fragments of the DSC heating traces (10 °C/min) indicating the glass transition in the grafted polymers taking place in the temperature range corresponding to the glass transition temperature of the bulk PBA

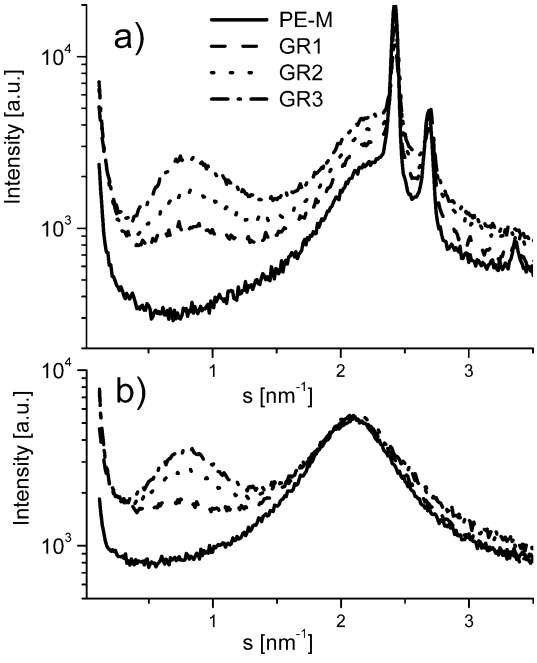

Fig. 5a,b X-ray diffraction intensity distributions recorded at: **a** room temperature; **b** 170 °C for the bulk samples of the macroinitiator and for grafted copolymers with various lengths of the PBA side chains

of the polyethylene are presented in Fig. 6. Two extreme cases can at first be considered: (1) the PE macroinitiator sample at room temperature for which the SAXS intensity maximum indicates the periodicity related to the semi-crystalline structure and (2) the sample with the longest PBA grafts for which the intensity maximum detected at the temperature above the melting point of PE indicates the microphase separation also when both constituents are molten. The correlation periods corresponding to the amorphous/crystalline and constitutional heterogeneities are only slightly different and can

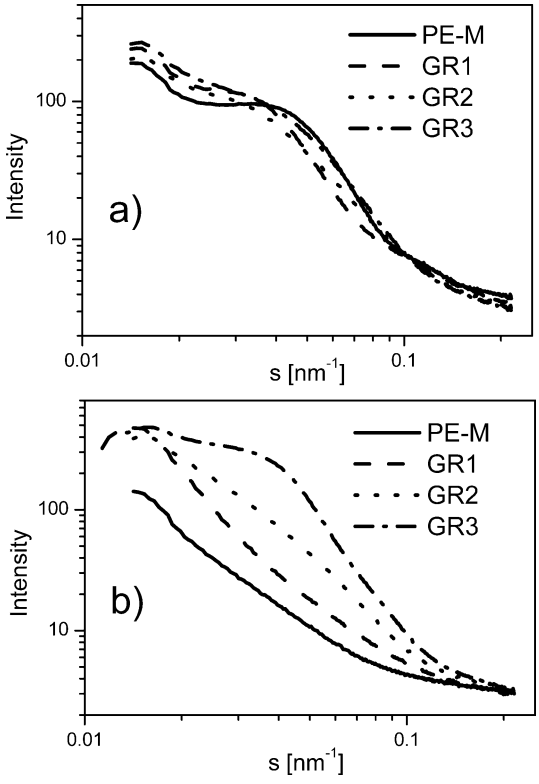

Fig. 6a,b SAXS intensity distributions recorded for the bulk polymers: **a** at room temperature; **b** at 150 °C

be estimated as Lc = 25 nm and Lh = 30 nm, respectively. All other samples constitute intermediate cases in which both periodicities contribute to the small angle scattering effect and the similarity of them does not allow any separation of the effects. Because of that, any precise conclusions concerning types of morphology and a comparison with related theories [38, 39] is impossible.

Viscoelastic properties of the studied materials have been characterized by means of the small amplitude dynamic deformation tests performed at a constant deformation frequency (10 rad/s) as a function of temperature. Results are presented in Fig. 7. They describe the mechanical behavior of the studied materials in all phases separated by the also here clearly seen transitions, i.e., the glass transition of the PBA phase and the melting in the PE phase. The first can be localized by the maximum of the G″ which appears for all grafted polymers at almost the same temperature, nearly −43 °C, in agreement with the DSC results. The second transition, the melting, is seen as a sharp drop of the both moduli (G′ and G″) at temperatures above 100 °C. In each phase the grafted components involve specific effects. Below the glass transition the PBA phase seems to play a role of reinforcement in the PE matrix so that the modulus of the material can even exceed the values determined for the pure polyethylene. Above the glass

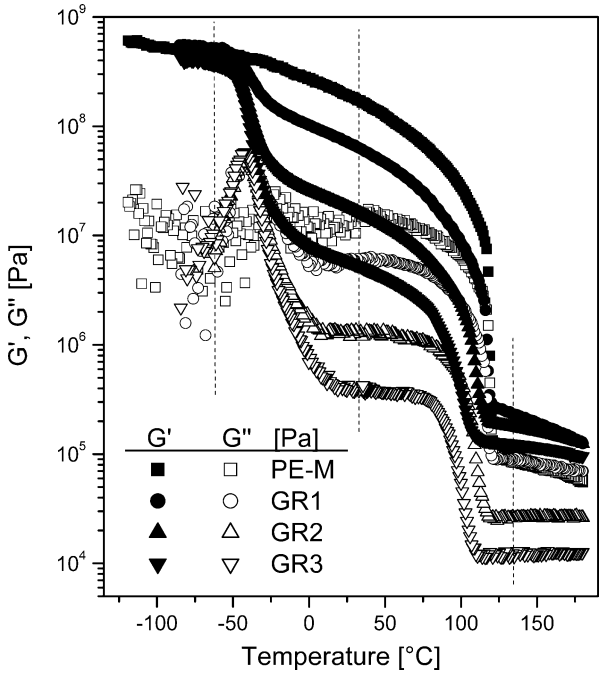

Fig. 7 Temperature dependencies of the real (G′) and imaginary (G″) shear modulus. Measured under small amplitude constant deformation frequency (10 rad/s) during cooling of samples with the rate of 2 °C/min

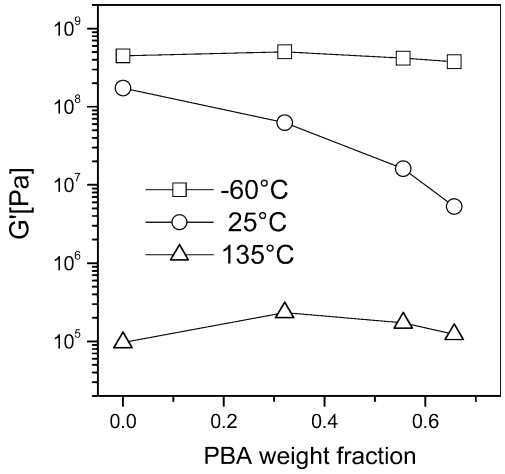

Fig. 8 Composition dependence of the real part of the shear modulus at various temperatures corresponding to different phases

transition of the PBA, the soft phase of grafts influences remarkably the modulus of the polymers to a degree dependent on composition. Variations of the shear modulus (Table 3) of the examined materials at various phases including the room temperature are shown in Fig. 8 as a function of composition. A strong effect of the presence of the grafted chains is also seen in the molten state in which the grafted polymers behave as elastomers with remarkably higher moduli than determined for the entangled polyethylene. Figure 8 shows also the modulus values determined at 135 °C. The observed behavior should be related to the two-phase structure of the systems with PBA microdomains probably dispersed in the PE matrix and networked by the PE backbone chains.

Behavior of the polymers under large deformation is illustrated in Fig. 9 by means of the stress-strain dependencies recorded during drawing the films at room temperature. The polyethylene sample is regarded as a reference. In this polymer the deformation is inhomogeneous at larger extensions and goes on by formation of a neck at the yield point and subsequent propagation of neck edges throughout the whole sample. This indicates a plastic deformation within the neck edges and a transformation of the non-oriented semicrystalline structure to a highly oriented one. The same transformation takes place in the sample with short grafts, however with the difference that the deformation is homogeneous on the macroscopically visible scale. The yield point parameters and the plastic flow stresses are in this sample much lower than in the PE reference. The elongation to break in the grafted polymer is slightly higher than in the PE sample. Table 4 shows all mechanical parameters which were determined for the studied samples in accordance to the scheme shown in Fig. 1. The polymers with long grafts exhibit a weak mechanical strength and break at relatively low extensions.

Such behavior can be well understood when the details of the structure are considered. As long as the grafted chains are short and correspondingly the fraction of the PBA phase is small, the polyethylene constitutes probably a continuous phase which under extensional deformation flows plastically which, in a similar way to the polyethylene, can leads to strong chain orientation and rearrangements in the crystalline

Table 3 Influence of composition on the shear modulus of the grafted copolymers at various temperatures belonging to different phases (compare with Figs. 7 and 8)

Sample	PBA fraction	G′(⁻60 °C) [MPa] (Below T_g)	G′(25 °C) [MPa] (Between T_g and T_m)	G′(135 °C) [MPa] (Above T_m)
PE-M	0	447	173	0.097
GR1	0.321	506	62	0.234
GR2	0.556	418	16	0.172
GR3	0.657	377	5.3	0.123

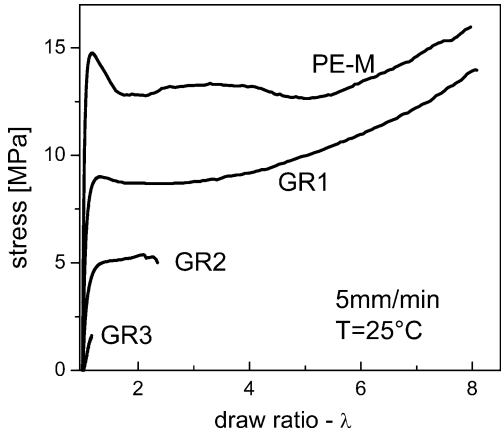

Fig. 9 Tensile stress-strain dependencies recorded during room temperature drawing of the grafted copolymer films (drawing rate of 1.0/min was used)

morphology. Indeed, the room temperature deformation of the polyethylene with short PBA grafts leads to uniform highly oriented materials with the crystalline phase which spans the highly oriented backbone chains. A comparison of the X-ray diffraction patterns and the SAXS patterns for the oriented states of PE and GR1 samples is shown in Fig. 10. The small angle patterns indicate strongly fibrillated materials.

The situation changes when the grafted chains become longer. For samples with longer grafted chains the highly oriented states were not achieved by drawing at room temperature because of probably phase inversed morphology in these samples. An illustration of morphologies supposed for the grafted copolymers on the bases of the results reported here is shown in Fig. 11 for the two characteristic cases: (1) short and (2) long grafted branches.

In the first case, the short grafted chains are arranged in microdomains dispersed in polyethylene matrix which, below the melting point, is physically cross-linked by the crystalline elements. Under tensile stresses the matrix will undergo deformation characteristic for the polyethylene. On the other hand, when the grafted chains become long the structural phase inversion can take place and the grafted chains will constitute the matrix. Such structure will be very weak for tensile

Table 4 Parameters characterizing the mechanical properties of films drawn at room temperature. Meaning of the determined parameters is illustrated in Fig. 1

Sample	$<E>$ [MPa]	$<\sigma_y>$ MPa	$\epsilon_y = <\lambda_y> - 1$	$<\sigma_B>$ MPa	λ_B
PE-M	362	14.8	0.148	13.9	4.4116
GR1	139	9.0	0.317	13.7	7.8473
GR2	56.9	5.1	1.717	5.06	1.8228
GR3	12.5			1.47	1.1501

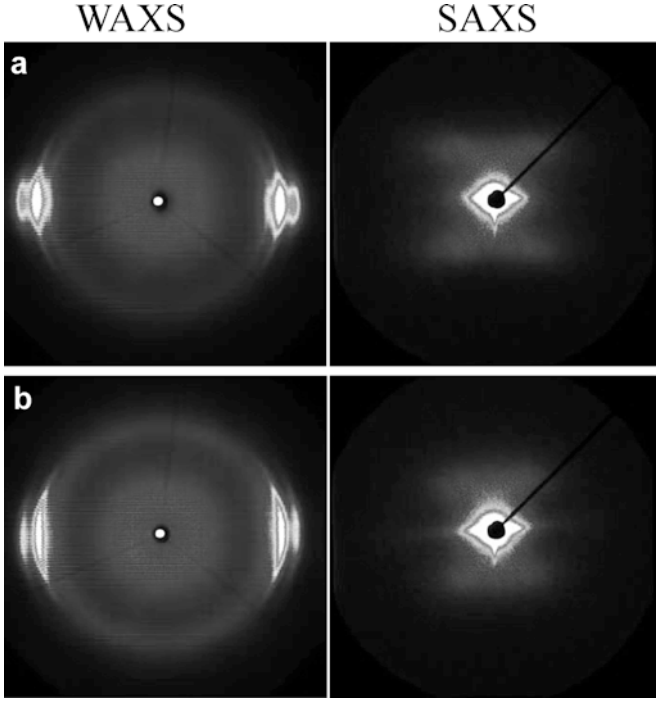

Fig. 10a,b X-ray diffraction and SAXS patterns for: **a** the PE-M samples; **b** the GR1 samples drawn to extensions exceeding $\lambda = 6$

deformation because the matrix can resist tensile forces only within the time necessary for disentanglement of the chains. This does not exclude, however, the relatively high modulus which such system can have when subjected to shear deformation. The later may be related to structural stability of the system when detected with small deformations.

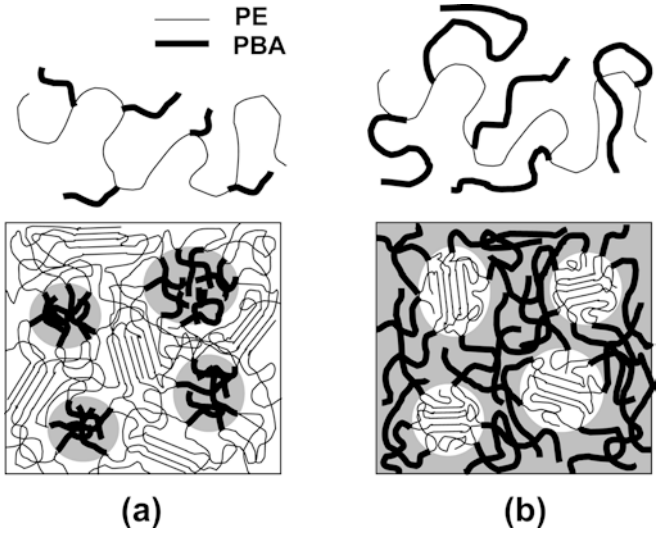

Fig. 11a,b Schematic illustration of morphologies expected for the grafted copolymers in two cases of: **a** short; **b** long grafted chains

Conclusions

The results presented have demonstrated a possibility of well controlled modification of polyethylene by converting the linear chains to multifunctional macroinitiators for the ATRP and allowing decoration of the PE chains by PBA grafted blocks. In this way, interesting block copolymer systems of amorphous-crystalline components have been obtained. Variation of polymer composition allowed a direct control of crystallinity of such systems and consequently a control of structure and properties in bulk. The analysis of structure has indicated a strong incompatibility of the components which in the studied range of compositions were able to preserve to some extent their individual properties, such as temperatures of transitions, even within the microphase separated structures of domain sizes not exceeding 50 nm scale. Large difference in properties of copolymer constituents resulted in a broad variation of properties of the copolymers with composition, especially in the temperature range between the glass transition of the PBA and the melting point of PE where the variation of shear modulus of samples by orders of magnitude was detected. The materials with predominant content of PE preserved a good extensibility as well as molecular and structural orientability constituting probably an interesting fiber forming product. The drastic loss of resistance to tensile deformation with increase of the length of the grafted chains is attributed to structural phase inversion which for the specific chain architecture is related to drastic change of system topology. This effect must not necessary be considered as a disadvantage but can become useful when the grafted chains will have another chemical nature or another property [40, 41] is considered. Therefore, further studies of related systems are in progress.

Acknowledgments We greatly appreciate the financial support from Mitsui Chemicals, the National Science Foundation (DMR-0090409), CRP Consortium at Carnegie Mellon University, and the Bundesministerium für Bildung, Forschung und Technologie (WTZ-Project POL 01/048). Dr. Norio Kashiwa and Tomoaki Matsugi are acknowledged for the donation of the PE-macroinitiator.

References

1. Chung TC (2002) Prog Polym Sci 27:39–85
2. Yanjarappa MJ, Sivaram S (2002) Progr Polym Sci 27:1347–1398
3. Matyjaszewski K (ed) (1998) Controlled radical polymerization. ACS Symposium Series, vol 685. American Chemical Society, Washington DC
4. Matyjaszewski K (ed) (2000) Controlled/living radical polymerization progress in ATRP, NMP, and RAFT. ACS Symposium Series, vol 768. American Chemical Society, Washington DC
5. Matyjaszewski K (ed) (2003) Advances in controlled/living radical polymerization. ACS Symposium Series, vol 854. American Chemical Society, Washington DC
6. Matyjaszewski K, Davis TP (eds) (2002) Handbook of radical polymerization. Wiley Interscience, Hoboken
7. Wang J-S, Matyjaszewski K (1995) J Am Chem Soc 117:5614–5615
8. Wang J-S, Matyjaszewski K (1995) Macromolecules 28:7901–7910
9. Patten TE, Xia J, Abernathy T, Matyjaszewski K (1996) Science 272:866–868
10. Matyjaszewski K, Xia J (2001) Chem Rev 101:2921–2990
11. Kamigaito M, Ando T, Sawamoto M (2001) Chem Rev 101:3689–3745
12. Patten TE, Matyjaszewski K (1998) Adv Mater 10:901–915
13. Patten TE, Matyjaszewski K (1999) Acc Chem Res 32:895–903
14. Matyjaszewski K (1999) Chem Eur J 5:3095–3102
15. Coessens V, Pintauer T, Matyjaszewski K (2001) Prog Polym Sci 26:337–377
16. Qiu J, Charleux B, Matyjaszewski K (2001) Prog Polym Sci 26:2083–2134
17. Pyun J, Matyjaszewski K (2001) Chem Mater 13:3436–3448
18. Matyjaszewski K, Pyun J, Gaynor SG (1998) Macromol Rapid Commun 19:665–670
19. Davis KA, Matyjaszewski K (2002) Adv Polym Sci 159:2–166
20. Coca S, Matyjaszewski K (1997) J Polym Sci Part A Polym Chem 35:3595–3601
21. Matyjaszewski K, Saget J, Pyun J, Schlogl M, Rieger B (2002) J Macromol Sci Chem A39:901–913
22. Matsugi T, Kojoh S-I, Kawahara N, Matsuo S, Kaneko H, Kashiwa N (2003) J Polym Sci Part A Polym Chem 41:3965–3973
23. Inoue Y, Matyjaszewski K (2004) J Polym Sci Part A Polym Chem 42:496–503
24. Coca S, Paik H-J, Matyjaszewski K (1997) Macromolecules 30:6513–6516
25. Bielawski CW, Morita T, Grubbs RH (2000) Macromolecules 33:678–680
26. Hong SC, Pakula T, Matyjaszewski K (2001) Macromol Chem Phys 202:3392–3402
27. Matyjaszewski K, Teodorescu M, Miller PJ, Peterson ML (2000) J Polym Sci Part A Polym Chem 38:2440–2448
28. Matyjaszewski K, Gaynor SG, Coca S (1998) PCT Int Appl WO 9840415
29. Liu S, Sen A (2001) Macromolecules 34:1529–1532
30. Schulze U, Fonagy T, Komber H, Pompe G, Pionteck J, Ivan B (2003) Macromolecules 36:4719–4726
31. Hong SC, Jia S, Teodorescu M, Kowalewski T, Matyjaszewski K, Gottfried AC, Brookhart M (2002) J Polym Sci Part A Polym Chem 40:2736–2749
32. Bowden NB, Dankova M, Wiyatno W, Hawker CJ, Waymouth RM (2002) Macromolecules 35:9246–9248
33. Inoue Y, Matsugi T, Kashiwa N, Matyjaszewski K (2004) Macromolecules (submitted)
34. Kashiwa N, Matsugi T, Kojoh S-I, Kaneko H, Kawahara N, Matsuo S, Nobori T, Imuta J-I (2003) J Polym Sci Part A Polym Chem 41:3657–3666
35. Matyjaszewski K, Patten TE, Xia J (1997) J Am Chem Soc 119:674–680
36. Gromada J, Matyjaszewski K (2002) Polym Prepr 43:195–196

37. Brandrup J, Immergut EH (1989) Polymer handbook. Wiley, New York, p V15
38. Qi S, Chakraborty AK, Wang H, Lefebvre AA, Balsara NP, Shakhnovich EI, Xenidou M, Hadjichristidis N (1999) Phys Rev Lett 82:2896
39. Qi S, Chakraborty AK (2001) J Chem Phys 115:3401–3405
40. Kwon OH, Nho YC, Perk KD, Kim YH (1999) J Appl Polym Sci 71:631–641
41. Geresh S, Gdalevsky GY, Gilboa I, Voorspoels J, Remon JP, Kost J (2004) J Controlled Release 94:391–399